Ceramics-Silikáty 67 (2), 246-251 (2023)
www.ceramics-silikaty.cz doi: 10.13168/cs.2023.0023

EFFECT OF Y_2O_3 ON THE STRUCTURE, THERMAL STABILITY AND ELASTIC MODULUS OF MAGNESIUM ALUMINOSILICATE GLASSES

XU ZHAOZHI*; TANG ZHIYAO**; LI YONGYAN**; YUE YUNLONG*; #KANG JUNFENG*

*School of Materials Science and Engineering, University of Jinan, Jinan, 250000, China
**Taishan Fiberglass Inc. (CTG), Tai'an, 271000, China

#E-mail: mse_kangjf@ujn.edu.cn

Submitted May 15, 2023; accepted June 19, 2023

Keywords: Y_2O_3, Elastic modulus, Glass structure, Thermal properties

The structure, thermal stability and elastic modulus of MgO–Al_2O_3–SiO_2 glasses doped with Y_2O_3 were studied by using XRD, FT-IR, density, DSC, and elastic modulus tests. The results showed that the glass samples remained amorphous with the addition of Y_2O_3. Moreover, the FT-IR results indicated that with an increase in the Y_2O_3 content, the overall change in the degree of polymerisation of the glass network structure showed an increasing trend. The T_g and first crystallisation peak T_{p1} of the glasses significantly increased, and the thermal stability was enhanced. As the Y_2O_3 content increased, the densities of the glasses increased from 2.59 g·cm^{-3} to 2.88 g·cm^{-3}. At the same time, the elastic modulus of glasses increased from 98.06 GPa to 107.77 GPa.

INTRODUCTION

High-modulus glass fibre is an important reinforcing material in composites. Unlike ordinary alkali free E glass fibre, high modulus glass fiber has the distinct features of having high tensile strength and an elastic modulus, good impact resistance, chemical stability and high temperature resistance [1], and is widely used in large wind blades, cable reinforcement cores, aircraft parts, automobile manufacturing, temperature resistant materials, sports equipment and other fields [2].

Currently, S-series fibreglass in the United States, Advantex fibreglass, HiPer-tex fibreglass in Europe, T-fibreglass in Japan, R-fibreglass in France, and ВМП Glass fibre in Russia and China's HS series glass fibre are the leading high-strength and high modulus glass fibre products in the market, with most of their main matrix components belonging to the silicon aluminium magnesium series or silicon aluminium magnesium calcium series [3]. However, it should be emphasised that MgO–Al_2O_3–SiO_2 glass itself has problems, such as a high upper limit of the crystallisation temperature, a fast crystallisation rate, a high melt viscosity, and difficulty in clarifying the glass liquid. Therefore, in production, it is generally necessary to introduce clarifying agents and fluxes to improve the process stability.

Many studies have shown that adding rare earth oxides can effectively reduce the melting and forming temperatures of glasses. Kang Junfeng et al. [4] found that doping the rare earth oxides (Y_2O_3, Er_2O_3 and La_2O_3) into the boro-aluminosilicate glass helped to decrease the melting temperature and viscosity. Wang Mitang et al. [5] found that solely doping Gd_2O_3 or Y_2O_3 with a content of 0.25-1.00 mol. %, and simultaneously doping Gd_2O_3 and Y_2O_3 with a total content of 1.00 mol. % into the Na_2O–CaO–SiO_2 system glass increased the coefficient of thermal expansion and decreased the glass melting temperature. Zheng Weihong et al. [6] suggested that the introduction of yttria effectively decreased the melting temperature and viscosity of lithium aluminosilicate glasses.

However, there is relatively little research on the rare earth elements' influence of on the elastic modulus of glasses. This article mainly studied the effects of yttrium oxide doping on the structure, density, thermal stability, and elastic modulus of glasses, thus attempting to develop a high-performance high modulus glass fibre.

EXPERIMENTAL

Glass preparation

In this paper, high modulus aluminosilicate glasses doped with different Y_2O_3 contents were prepared and studied. The glasses chemical compositions are listed in Table 1, in which glass samples were numbered as Y1 to Y5 with the increasing addition of Y_2O_3. The raw materials were all chemically pure substances. The glass batches were uniformly mixed and then placed into a platinum crucible, then melted in a furnace with the

temperature of 1550-1600 °C for 4 hours. The bubble free and homogeneous glassy melt was poured into a graphite mould to obtain the glass block. Subsequently, the formed glass was transferred to a muffle furnace at a temperature near T_g for 1 h to eliminate the stress. The structure and properties of the obtained parent glasses were tested after the sample preparation.

Table 1. Chemical compositions of the glass samples with the different Y_2O_3 content (mol. %).

Sample	SiO_2	MgO	Al_2O_3	TiO_2	Y_2O_3
Y1	60	20	15	5	0
Y2	60	20	15	5	1.2
Y3	60	20	15	5	2.4
Y4	60	20	15	5	3.6
Y5	60	20	15	5	4.8

Characterisation

To confirm that the basic glass was amorphous, the annealed glass powder was analysed by an X-ray diffractometer (XRD, D8-ADVANCE, Bruker, Germany). The test was performed with a scanning speed 10 °·min^{-1} with 2θ = 10° to 80° using Cu Kα radiation, under the working voltage of 60 kV and the working current of 200 mA.

The glass structure was analysed by the Fourier transform infrared spectrum (FT-IR, Nicolet iS 10, Thermo Scientific, the United States) with the wavenumber of 400-1400 cm^{-1}. The sample preparation method was to mix and grind the glass powder and KBr at a weight ratio of 1:100 with a particle size less than 2.5 μm. The ground mixture was poured into a mould and pressed to a transparent sheet under 15 MPa. Finally, the analyser scanned the slice 32 times to obtain the absorption spectrum.

The density measurement was based on Archimedes' principle, using a density analyser at room temperature with distilled water. To increase the accuracy, each sample was measured three times to obtain the average value of the measured density.

Glass powder was used for the thermal analysis by differential scanning calorimetry (DSC, DSC 404F3, Netzsch, Germany). The test temperatures ranged from 200 °C to 1200 °C with a heating rate 10 °C·min^{-1}.

In this paper, the elastic modulus was tested by an intrinsic mechanics measuring instrument (Xuhui Xinrui Technology Co., LTD, China). The glass sample was fixed on the test equipment and the size information of the glass sample was set. Then one end of the sample to be tested was tapped to obtain the vibration signal which was automatically collected by the instrument, and the corresponding software automatically calculated the elastic modulus value. The size of the glass sample with a polished surface was 60 × 12 × 3 mm. Each group of samples was measured three times and the average value was adopted.

RESULTS AND DISCUSSION

XRD analysis

The XRD results of the glass samples with the different Y_2O_3 content are shown in Figure 1. It can be seen from the figure that the diffraction patterns for the Y1 to Y5 samples were all dispersion peaks, and no sharp characteristic peaks were observed, which indicated that the prepared glasses were all in an amorphous state [7].

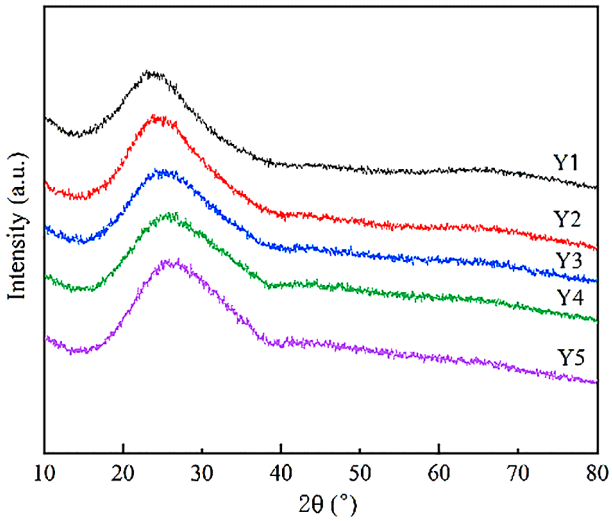

Figure 1. XRD results of the parent glass samples with the different Y_2O_3 content.

FT-IR analysis

The FT-IR spectrum of the Y1-Y5 samples shows absorption bands from 400 to 1500 cm^{-1}, as shown in Figure 2 From the absorption spectrum, it can be seen that there were five characteristic absorption peaks. The first absorption peak located at 450 cm^{-1} was caused

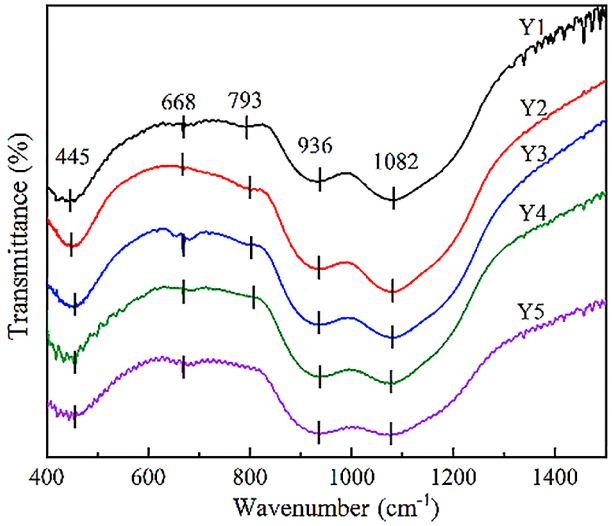

Figure 2. FT-IR results of the glass samples with the different Y_2O_3 content.

by the symmetric stretching vibration of Si–O–Si (b) [8], and the absorption peak generally moved towards a low wave number direction. Al^{3+} ions act as a glass network modifier, combining with the non-bridging oxygen (NBO) atoms to form [AlO_4] tetrahedra or [AlO_6] octahedra. The vibration corresponding to wave number of Si–O–Al connected by the [SiO_4] tetrahedra and [AlO_4] tetrahedra was around 668 cm^{-1} [9]. Since Si/Al was not changed in this experiment, it can be seen from the optical spectrum that it remained basically unchanged. The third absorption peak located at 793 cm^{-1} was generated by the symmetric stretching vibration in the [AlO_4] tetrahedron [10], and it can be seen that its absorption peak shifted towards a higher wave number.

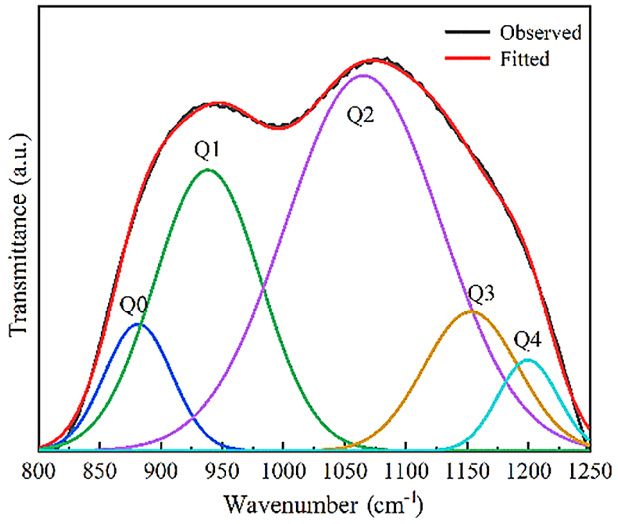

Figure 3. Deconvoluted IR spectrum at 800-1250 cm^{-1} of the glass doped with the different Y_2O_3 content.

The relatively wide absorption band at a wavelength of 800-1250 cm^{-1} is the bridging oxygen Q_n formed by the Si–O bond of the [SiO_4] tetrahedron and the different numbers of [SiO_4] tetrahedrons (n = 0, 1, 2, 3, and 4) [11]. The absorption peaks of 900-950 cm^{-1} in the spectrum corresponded to Si-O-Si stretching vibrations or non-bridging oxygen vibrations, while the absorption peaks at 1050-1120 cm^{-1} are connected to antisymmetric stretching vibrations or Si–O–Si stretching vibrations of the bridging oxygen. To better analyse the changes in the glass network structure with the increasing Y_2O_3 content, deconvolution fitting was performed at 800-1250 cm^{-1}. The infrared spectrum of sample Y4 fitted with Gaussian distribution is shown in Figure 3. The frequencies (Vi) and the relative areas (Ai) of the FT-IR bands obtained from the deconvolution fits are shown in Table 2. The centres of the five fitted curves are 881, 938, 1065, 1153, and 1199 cm^{-1}, corresponding to Q_0, Q_1, Q_2, Q_3, and Q_4, respectively. As Y_2O_3 increased, the centres of the five fitted curves moved towards lower wavenumbers. The relative areas of the peaks located at 881 and 938 increased from 5.2 % and 20.0 % to 7.6 % and 24.5 %, respectively. At the same time, the relative areas of the 1065 cm^{-1} peak corresponding to Q_2 decreased from 62.9 % to 42.8 %. The relative area changes of the corresponding peaks for Q_3 and Q_4 first decreased from 8.9 % and 2.9 % to 8.3 % and 2.8 %, respectively, and then significantly increased to 18.0 % and 7.1 %, respectively. Through the peak fitting results, it is clear that with the increase in the Y_2O_3 content, Q_2 transformed into Q_3 and Q_4, first leading to a decrease in the degree of polymerisation of the glass network and then an increase. At the same time, combined with the overall trend of the changes, the degree of polymerisation of the glass network showed a general increasing trend. In addition, the increasing amount of Y_2O_3 in some aluminosilicate glasses has promoted the creation of more BO in the glassy matrix [12]. Shakeri and Rezvani considered that the Y^{3+} ions played the role of network forming ions in the presence of tetrahedrally coordinated Al^{3+} ions [13]. Therefore, with the increase in the yttrium oxide content, the degree of network polymerisation of the glass network increased.

Table 2. Frequencies (Vi) and the relative areas (Ai) of FT-IR bands obtained from the deconvolution fits.

Sample	Y1	Y2	Y3	Y4	Y5
V_0 (cm^{-1})	884.3	882.7	881.2	881.5	875.7
V_1 (cm^{-1})	933.2	934.1	936.0	938.3	930.8
V_2 (cm^{-1})	1076.3	1073.0	1069.3	1065.3	1041.6
V_3 (cm^{-1})	1170.4	1167.6	1160.1	1153.1	1128.7
V_4 (cm^{-1})	1208.9	1206.8	1203.6	1199.6	1192.3
A_0 (%)	5.2	6.1	7.1	7.4	7.6
A_1 (%)	20.0	22.4	24.7	25.9	24.5
A_2 (%)	62.9	60.4	54.19	50.5	42.8
A_3 (%)	8.9	8.3	10.0	11.4	18.0
A_4 (%)	2.9	2.8	4.1	4.7	7.1

DSC analysis

Figure 4 displays the DSC curves of the Y1-Y5 glass samples. From the results, it shows that the glass transition temperature T_g increased from 755 °C to 774 °C as the Y_2O_3 content increased. The Y1 sample had two crystallisation peaks, at 904 °C and 1169 °C, respectively. With the increase in the Y_2O_3 content, the first crystallisation temperature T_{p1} increased from 904 to 999 °C, while the second crystallisation peak first showed a decreasing trend and then an increasing one, reaching a minimum value of 1064 °C in the Y4 sample. Different concentrations of Y_2O_3 can lead to differences in the glass structure and crystallisation energy barriers. During the crystallisation process, the rearrangement of atoms must overcome the energy barriers, ultimately leading to the different crystallisation abilities of the sample, which are reflected in the crystallisation tem-

perature. The first crystallisation peak became more moderate, indicating the increasing thermal stability of the glass. Based on the infrared spectroscopy testing results, it can be seen that the overall degree of the glass network aggregation increased with the addition of Y_2O_3, and the connections in the [SiO_4] tetrahedra became better. Moreover, due to the Y^{3+} ions' large field strength, it can strengthen network structure to improve the integrity of the glass structure. This ultimately leads to an increase in the glass viscosity.

In many cases, the nucleation and growth of crystals were closely related to the diffusion, which depended on the viscosity. The Stokes-Einstein equation can effectively reveal the relationship between the diffusion coefficient D and the viscosity η: $D = k_BT/6\pi r\eta$, where k_B is the Boltzmann constant, T is the absolute temperature, and r is the moving article radius [14]. In summary, as the content of yttrium oxide increased, the viscosity of the glass gradually increased, which hindered the orderly arrangement of atoms and, thus, inhibited the precipitation of crystals. Therefore, the intensity of the first crystallisation peak significantly decreased.

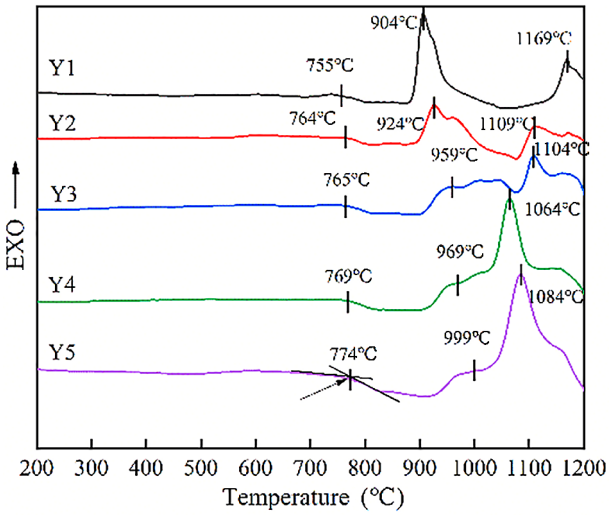

Figure 4. DSC results of the glass samples with the different Y_2O_3 content.

The glass thermal stability can be qualitatively understood by Dietzel's thermal stability ($\Delta T = (T_{p1} - T_g)$ [15]. It can be calculated from the correlation temperatures obtained in the DSC results in Figure 5, which can effectively reflect the ability of the material against crystallisation. The higher value of ΔT means that the greater the thermal stability, which may due to the delay of the nucleation process. From the figure, it can be seen that with the increase of Y_2O_3 content, the ΔT value increased from 149 °C to 225 °C, indicating the significant enhancement of the thermal stability of the glass samples [16]. In addition, when ΔT is greater than 100; The glass has greater thermal stability and can be used in the fibre drawing process [17].

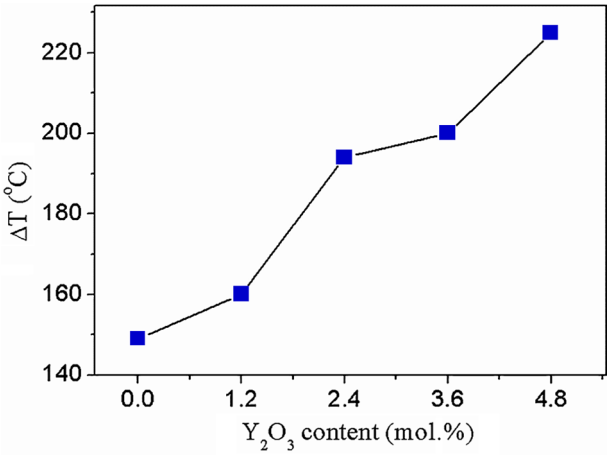

Figure 5. Thermal stability of the glass samples with the different Y_2O_3 content.

Density analysis

The density is a fundamental parameter that characterises the macroscopic structure of glass, and its influencing factors mainly depend on the atomic molar mass of the glass and the network structure of the glass. Figure 6 displays the density of magnesium aluminium silicate glasses with the different Y_2O_3 content. The results showed that the densities of the samples increased from 2.59 to 2.88 g·cm^{-3}. Fundamentally, firstly, the relative atomic mass of Y is larger than that of other atomic masses in the glass, which significantly increased the density of the glass as its content increased. At the same time, from the infrared spectrum, it can be seen that the overall polymerisation degree of the silicon oxide network in the glass structure increased with the increasing Y_2O_3 content, and the integrity of the network showed an increasing trend. The increase in the relative molecular weight of the glass combined with the increase in the polymerisation degree of the glass network led to a linear increase in the glass density with the increase in the Y_2O_3 content.

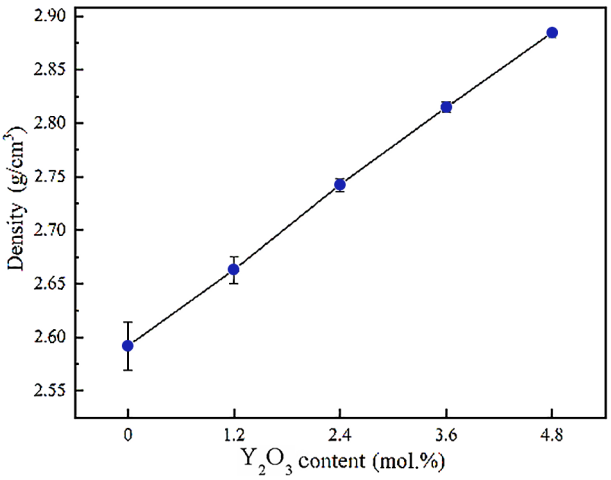

Figure 6. Densities of the glass samples with the different yttrium oxide content.

Elastic modulus analysis

Figure 7 shows the elastic modulus of the Y1-Y5 glass samples. It is clear that with the increase in the Y_2O_3 content, the glass elastic modulus (E) increased from 98.06 to 107.77 GPa. The E is directly connected to the strength of the chemical bonds in the glass structure. Glass samples with stronger chemical bonds have a larger elastic modulus. Due to the large field strength of the Y^{3+} ions, they accumulated free oxygen outside the network, which greatly promoted the improvement in the elastic modulus. In addition, with the increase in the yttrium oxide content, the degree of network polymerisation of the glass network increased, which led to the elastic modulus gradually increasing.

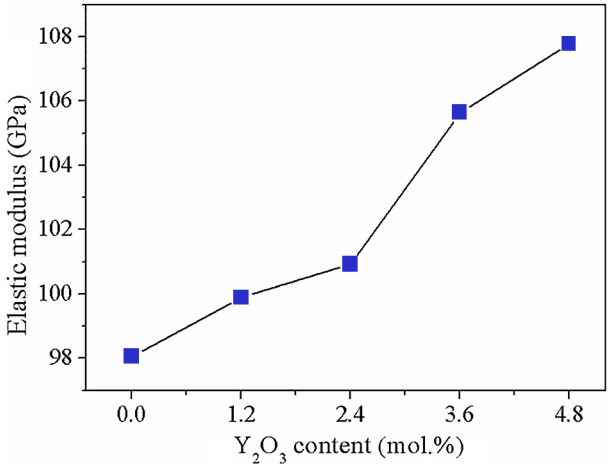

Figure 7. Elastic modulus of the glass samples doped with the different yttrium oxides.

CONCLUSIONS

In this work, the structure, thermal stability, and elastic modulus of $MgO–Al_2O_3–SiO_2$ glasses doped with Y_2O_3 were systematically studied. From the experimental results, it is clear that after adding Y_2O_3, all the glass samples remained amorphous. Moreover, the FT-IR results indicated that with the increase in the Y_2O_3 content, the overall change in the degree of polymerisation of the glass network structure showed an increasing trend. With the increase in the Y_2O_3 content, the T_g and first crystallisation peak T_{p1} increased from 755 °C and 904 °C to 774 °C and 1169 °C, respectively. Furthermore, the values of the parameter ΔT increased from 149 °C to 225 °C, which indicated the thermal stability of the glass samples was enhanced. As the Y_2O_3 content increased, the densities of the glasses increased from 2.59 g·cm^{-3} to 2.88 g·cm^{-3}. Meanwhile, the elastic modulus of the glass increased from 98.06 GPa to 107.77 GPa.

Acknowledgements

This paper was supported by the National Natural Science Foundation of China (No. 52172019 and No. 52072148), the Natural Science Foundation of Shandong Province (No. ZR2019BEM002), and the Opening Project of State Key Laboratory of Advanced Technology for Float Glass (No. 2020KF01).

REFERENCES

1. Messier D. R., Patel P. J. (1995): High modulus glass fibers. *Journal of Non-Crystalline Solids*, *182*(3), 271-277. doi: 10.1016/0022-3093(94)00520-6
2. Li H., Richards C., Watson J. (2014): High-performance glass fiber development for composite applications. *International Journal of Applied Glass Science*, *5*(1), 65-81. doi: 10.1111/ijag.12053
3. Zu Q., Huang S., Zhang Y., Huang S., Liu J., Li H. (2017): Compositional effects on mechanical properties, viscosity, and crystallization of (Li_2O, B_2O_3, MgO)–Al_2O_3–SiO_2 glasses. *Journal of Alloys and Compounds, 728, 552-563.* doi: 10.1016/j.jallcom.2017.08.294
4. Hou Y., Cheng J., Kang J., Yuan J., Cui J. (2018): Structure, glass stability and rheological properties of Na_2O–CaO––Al_2O_3–SiO_2 glasses doped with Y_2O_3. *Ceramics-Silikáty, 62(2), 173-180.* doi: 10.13168/cs.2018.0009
5. Wang M., Cheng J., Li M., He F., Deng W. (2012): Viscosity and thermal expansion of soda-lime-silica glass doped with Gd_2O_3 and Y_2O_3. *Solid State Sciences*, *14*(8), 1233-1237. doi: 10.1016/j.solidstatesciences.2012.06.001
6. Zheng W., Cheng J., Tang L., Jian Q., Cao X. (2007): Effect of Y_2O_3 addition on viscosity and crystallization of the lithium aluminosilicate glasses. *Thermochimica Acta*, 456, 69-74. doi: 10.1016/j.tca.2007.01.022
7. Zhang L., Qu Y., Wan X., Zhao J., Zhao J., Yue Y., Kang J. (2020): Influence of rare earth oxides on structure, dielectric properties and viscosity of alkali-free aluminoborosilicate glasses. *Journal of Non-Crystalline Solids*, *532*, 119886. doi: 10.1016/j.jnoncrysol.2020.119886
8. Annapurna K., Das M., Kundu P., Dwivedi R., N., (2005): Buddhudu, Spectral properties of Eu^{3+}: ZnO–B_2O_3–SiO_2 glasses. *Journal of molecular structure*, *741*(1-3), 53-60. doi: 10.1016/j.molstruc.2005.01.062
9. Hamilton J. P., Brantley S. L., Pantano C. G., Criscenti L. J., Kubicki J. D. (2001): Dissolution of nepheline, jadeite and albite glasses: toward better models for aluminosilicate dissolution. *Geochimica et Cosmochimica Acta*, *65*(21), 3683-3702. doi: 10.1016/S0016-7037(01)00724-4
10. Garai M., Sasmal N., Molla A. R., Tarafder A., Karmakar B. (2015): Effects of in-situ generated coinage nanometals on crystallization and microstructure of fluorophlogopite mica containing glass–ceramics. *Journal of Materials Science & Technology*, *31*(1), 110-119.doi: 10.1016/j.jmst.2014.11.012
11. Roy B.N. (1990): Infrared Spectroscopy of Lead and Alkaline-Earth Aluminosilicate Glasses. *Journal of the American Ceramic Society, 73(4), 846-855.* doi: 10.1111/j.1151-2916.1990.tb05124.x
12. Mahdy E.A., Ibrahim S. (2012): Influence of Y_2O_3 on the structure and properties of calcium magnesium aluminosi-

licate glasses. *Journal of Molecular Structure, 1027*, 81-86. doi: 10.1016/j.molstruc.2012.05.055

13. Shakeri M.S., Rezvani M. (2011): Optical band gap and spectroscopic study of lithium alumino silicate glass containing Y^{3+} ions, *Spectrochimica Acta Part A Molecular & Biomolecular Spectroscopy*, 79, 1920-1925. doi: 10.1016/j.saa. 2011.05.090
14. Kang J.F., Wang J., Cheng J.S., Yuan J., Hou Y.S., Qian S.Y. (2017): Crystallization behavior and properties of CaO––MgO–Al_2O_3–SiO_2 glass -ceramics synthesized from granite wastes. *Journal of Non-Crystalline Solids*, *457*, 111-115. doi: 10.1016/j.jnoncrysol.2016.11.030
15. Zhao J., Y. Lu, Kang J., Qu Y., Khater G.A., Li S., Wang Y., Yue Y. (2018): Effect of Y_2O_3 and La_2O_3 on structure and dielectric properties of aluminoborosilicate glasses. *Journal of Non-Crystalline Solids*, *496*, 1-5. doi: 10.1016/j.jnoncrysol.2018.05.020
16. Singh S., Kalia G., Singh K. (2015): Effect of intermediate oxide (Y_2O_3) on thermal, structural and optical properties of lithium borosilicate glasses. *Journal of Molecular Structure, 1086, 239-245.* doi: 10.1016/j.molstruc.2015.01.031
17. Zhang L., Kang J., Wang J., Khater G.A., Shi Q., Li S., Zhao J., Teng J., Yue Y. (2019): Effects of Y_2O_3 on structure and dielectric properties of aluminoborosilicate glasses. *Journal of Non-Crystalline Solids*, *503*, 110-114. doi: 10.1016/j.jnoncrysol.2018.09.032